JACC: CARDIOVASCULAR IMAGING VOL. 8, NO. 10, 2015

ISSN 1936-878X/$36.00
PUBLISHED BY ELSEVIER INC. http://dx.doi.org/10.1016/j.jcmg.2015.06.014

Predictors of Plaque Rupture Within Nonculprit Fibroatheromas in Patients With Acute Coronary Syndromes

The PROSPECT Study

Bo Zheng, MD,*†‡ Gary S. Mintz, MD,† John A. McPherson, MD,§ Bernard De Bruyne, MD, PhD,‖ Naim Z. Farhat, MD,¶ Steven P. Marso, MD,# Patrick W. Serruys, MD, PhD,** Gregg W. Stone, MD,*† Akiko Maehara, MD*†

ABSTRACT

OBJECTIVES The study sought to examine the relative importance of lesion location versus vessel area and plaque burden in predicting plaque rupture within nonculprit fibroatheromas (FAs) in patients with acute coronary syndromes.

BACKGROUND Previous studies have demonstrated that plaque rupture is associated with larger vessel area and greater plaque burden clustering in the proximal segments of coronary arteries.

METHODS In the PROSPECT (Providing Regional Observations to Study Predictors of Events in the Coronary Tree) study 3-vessel grayscale and radiofrequency-intravascular ultrasound was performed after successful percutaneous coronary intervention in 697 patients with acute coronary syndromes. Untreated nonculprit lesion FAs were classified as proximal (<20 mm), mid (20 to 40 mm), and distal (>40 mm) according to the distance from the ostium to the maximum necrotic core site.

RESULTS Overall, 74 ruptured FAs and 2,396 nonruptured FAs were identified in nonculprit vessels. The majority of FAs (73.6%) were located within 40 mm of the ostium, and the vessel area and plaque burden progressively decreased from proximal to distal FA location (both $p < 0.001$). In a multivariate logistic regression model, independent predictors for plaque rupture included the distance from the ostium to the maximum necrotic core site per millimeter (odds ratio [OR]: 0.86; 95% confidence interval [CI]: 0.76 to 0.98; $p = 0.02$), plaque burden per 10% (OR: 2.05; 95% CI: 1.63 to 2.58; $p < 0.0001$), vessel area per mm^2 (OR: 1.14; 95% CI: 1.11 to 1.17; $p < 0.0001$), calcium (OR: 0.09; 95% CI: 0.05 to 0.18; $p < 0.0001$), and right coronary artery location (OR: 2.16; 95% CI: 1.25 to 3.27; $p = 0.006$). By receiver-operating characteristic analysis, vessel area correlated with plaque rupture stronger than either plaque burden ($p < 0.001$) or location ($p < 0.001$).

CONCLUSIONS Large vessel area, plaque burden, proximal location, right coronary artery location, and lack of calcium were associated with FA plaque rupture. The present study suggests that among these variables, vessel area may be the strongest predictor of plaque rupture among non–left main coronary arteries. (PROSPECT: An Imaging Study in Patients With Unstable Atherosclerotic Lesions [PROSPECT]; NCT00180466) (J Am Coll Cardiol Img 2015;8:1180–7)

From the *New York-Presbyterian/Columbia University Medical Center, New York, New York; †Cardiovascular Research Foundation, New York, New York; ‡Peking University First Hospital, Beijing, China; §Vanderbilt University School of Medicine, Nashville, Tennessee; ‖Cardiovascular Center Aalst, OLV-Clinic, Aalst, Belgium; ¶North Ohio Heart Center/Elyria Memorial Hospital Regional Medical Center, Elyria, Ohio; #University of Texas Southwestern Medical Center, Dallas, Texas; and the **Erasmus Medical Center, Rotterdam, the Netherlands. Dr. Zheng has received a research grant from Boston Scientific. Dr. Mintz is a consultant for Volcano Corporation, Boston Scientific, InfraReDx, and ACIST; has received fellowship/grant support from Volcano Corporation, Boston Scientific, and InfraReDx; and has received honoraria from Boston Scientific, InfraReDx, and ACIST. Dr. McPherson has received consultant fees from Cardiox, Inc., Healthwise, Inc., and Velomedix Inc. Dr. De Bruyne's institution receives grant support and consulting fees on his behalf from St. Jude Medical. Dr. Marso is a consultant for St. Jude Medical, Novo Nordisk, and The Medicines Company; and has received research grants from Bristol-Myers Squibb, Novo Nordisk, Terumo, The Medicines Company, and Volcano Corporation. Dr. Maehara has received grant support from Boston Scientific; is a consultant for ACIST and Boston Scientific; and has received speaker fees from St. Jude Medical. All other authors have reported that they have no relationships relevant to the contents of this paper to disclose. H. Vernon Anderson, MD, served as Guest Editor for this paper.

Manuscript received March 18, 2015; revised manuscript received June 9, 2015, accepted June 14, 2015.

Previous pathologic studies have demonstrated that plaque rupture with thrombosis is the major mechanism leading to acute coronary syndromes (1-4). Lesions with high-risk characteristics, including thin-cap fibroatheromas (TCFAs) and plaque rupture, cluster predominantly in the proximal coronary segment of the left anterior descending artery (LAD) and more diffusely throughout the right coronary artery (RCA) (5-8). Vessel area, shear stress, and other anatomic features contribute to this pattern of longitudinal distribution (7-11); however, whether proximal location independently determines the risk of plaque rupture has remained unclear (7,8). The present study aims to investigate the predictors of plaque rupture among fibroatheromas within nonculprit lesions by using the 3-vessel grayscale and intravascular ultrasound (IVUS)-virtual histology (VH) data from the PROSPECT (Providing Regional Observations to Study Predictors of Events in the Coronary Tree) study.

SEE PAGE 1188

METHODS

PATIENT POPULATION AND PROTOCOL. The enrollment criteria and the methodology of the PROSPECT study have been previously described in detail (12). In brief, 697 patients with acute coronary syndromes underwent grayscale and IVUS-VH examination of the proximal 6 to 8 cm of all the 3 coronary vessels after successful percutaneous coronary intervention of culprit lesions and other severe stenoses. The study was approved by the institutional review board or medical ethics committee at each participating center, and all patients signed written informed consent (12). Of 697 patients enrolled in the PROSPECT study, 454 patients with at least 1 fibroatheroma in a nonculprit vessel comprised the current study population.

QUANTITATIVE ANALYSIS OF CORONARY ANGIOGRAPHY AND IVUS. Imaging was performed using a synthetic aperture array, 20 MHz, 3.2-F catheter (Eagle Eye, Volcano Corporation, Rancho Cordova, California). During a motorized catheter pullback at 0.5 mm/s, grayscale IVUS was recorded, and radiofrequency data were captured gated to the R-wave (In-Vision Gold, Volcano Corporation). Qualitative and quantitative coronary angiographic assessment of the entire length of the coronary tree was performed at an independent core laboratory (Cardiovascular Research Foundation, New York, New York) using a proprietary methodology modified from standard Medis CMS software version 7.0 (Leiden, the Netherlands); this analysis included each major epicardial coronary artery and every side branch >1.5 mm in diameter. This 3-vessel angiographic analysis served as a roadmap to identify each lesion on the basis of longitudinal axis location (mm). Detailed angiographic, grayscale, and IVUS-VH methodology have been described previously (13). All IVUS images were also analyzed at an independent core laboratory (Cardiovascular Research Foundation). Off-line grayscale and IVUS-VH analyses were performed using: 1) QCU-CMS (Medis) for contouring; 2) pcVH 2.1 software (Volcano Corporation) for contouring and data output; and 3) proprietary qVH software for segmental qualitative assessment and quantitative data output.

A lesion was defined as a segment with ≥3 consecutive frames with ≥40% plaque burden. A fibroatheroma was defined as >10% confluent necrotic core (NC) and was subclassified as TCFA-VH, calcified thick-cap fibroatheroma (CaThCFA), and non-CaThCFA (13). A plaque

ABBREVIATIONS AND ACRONYMS

AUC = area under the curve
CaThCFA = calcified thick-cap fibroatheroma
EEM = external elastic membrane
IVUS = intravascular ultrasound
LAD = left anterior descending artery
LCX = left circumflex artery
NC = necrotic core
RCA = right coronary artery
ROC = receiver-operating characteristic
TCFA = thin-cap fibroatheroma
VH = virtual histology

TABLE 1 Baseline Characteristics of Patients With Nonculprit Vessel Fibroatheromas

Age, yrs	58.6 (51.5–67.5)
Men	80.2 (364/454)
Diabetes mellitus	17.9 (81/452)
Insulin requiring	2.2 (10/452)
Metabolic syndrome	49.9 (221/443)
Current cigarette use	47.3 (211/446)
Hypertension	48.3 (218/451)
Hyperlipidemia	45.5 (190/418)
Prior myocardial infarction	11.3 (51/450)
Family history of coronary artery disease	46.1 (185/401)
Framingham score	7.0 (5.0–9.0)
Prior percutaneous coronary intervention	10.8 (49/453)
Clinical presentation	
ST-segment elevation myocardial infarction	29.5 (134/454)
Non–ST-segment elevation myocardial infarction	66.5 (302/454)
Unstable angina with electrocardiogram changes	4.0 (18/454)
Body mass index, kg/m^2	28.1 (25.4–31.6)
Total cholesterol, mg/dl	172.0 (148.0–200.0)
Low-density lipoprotein cholesterol, mg/dl	101.4 (80.2–129.6)
High-density lipoprotein cholesterol, mg/dl	38.6 (34.0–46.0)
Triglycerides, mg/dl	125.5 (88.6–177.1)
Hemoglobin A1c, %	5.8 (5.3–6.2)
Estimated creatinine clearance, ml/min	99.2 (75.3–125.4)
High-sensitivity C-reactive protein, mg/dl	7.7 (2.5–18.8)
Statin at admission	46.7 (212/454)
Aspirin at admission	72.7 (330/454)
Clopidogrel at admission	62.3 (283/454)
Number of diseased epicardial coronary arteries	
1	24.7 (110/446)
2	44.2 (197/446)
3	31.2 (139/446)

Values are median (interquartile range) or % (n/N).

rupture was defined as a cavity that communicated with the lumen with an overlying residual fibrous cap fragment.

One lesion could have multiple plaque ruptures (14). Rupture sites separated by ≥3 consecutive frames (approximately 1.5 mm) of artery containing smooth lumen contours and no cavity were considered to represent discrete and separate plaque ruptures.

One lesion could also contain more than 1 fibroatheroma. The main fibroatheroma groups (VH-TCFA, CaThCFA, and non-CaThCFA) required 3 consecutive slices demonstrating the same main fibroatheroma subtype. Fibroatheromas were considered multiple and distinct if they were separated by ≥3 consecutive image slices containing a different fibroatheroma subtype or nonfibroatheroma phenotype (13). The fibroatheroma subtype was assigned on the basis of the maximum NC slice. Plaque rupture was also mapped at the fibroatheroma level.

To evaluate the longitudinal distribution of IVUS-identified fibroatheromas, distances were measured from the ostium of the coronary artery to the slice with the greatest amount of NC within the fibroatheroma. Fibroatheromas were assigned to proximal (<20 mm), mid (20 to 40 mm), or distal segments (>40 mm) depending on the distance from the maximum NC site to the ostium of LAD, left circumflex artery (LCX), or RCA.

TABLE 2 Angiographic, Grayscale IVUS, and IVUS-VH Findings in Patients With Nonculprit Vessel Fibroatheromas

Patient-level findings	
Total length of angiographic nonculprit lesions, mm	20.3 (9.6–37.7)
Number of angiographic nonculprit lesions	2.0 (1.0–4.0)
Number of IVUS nonculprit lesions	5.0 (4.0–6.0)
Patients with ≥1 lesions with minimum lumen area ≤4 mm^2	55.9 (254/454)
Patients with ≥1 lesions with plaque burden ≥70%	35.9 (163/454)
Patients with ≥1 thin-cap fibroatheroma	63.7 (289/454)
Necrotic core volume, %	13.6 (9.0–18.7)
Dense calcium volume, %	5.9 (3.5–9.3)
Fibrous tissue volume, %	59.6 (55.5–63.7)
Fibrofatty volume, %	18.4 (13.7–24.5)
Lesion-level findings	
Minimum lumen area, mm^2	5.89 (4.33–8.10)
Minimum lumen area <4 mm^2	18.9 (451/2,382)
Plaque burden, %	56.0 (49.4–63.2)
Plaque burden ≥70%	9.2 (218/2,382)
Remodeling index	0.93 (0.84–1.00)
Necrotic core volume, %	13.1 (6.5–22.2)
Dense calcium volume, %	4.3 (1.2–9.7)
Fibrous tissue volume, %	60.6 (51.8–67.9)
Fibrofatty volume, %	16.0 (8.7–25.8)

Values are median (interquartile range) or % (n/N) for patient-level analysis; values are least squares means (95% confidence interval) or % (n) for lesion-level analysis..

IVUS = intravascular ultrasound; VH = virtual histology.

STATISTICAL ANALYSIS. Categorical variables are presented using frequencies and percentages and compared using chi-square statistics, and continuous variables are presented as median (interquartile range) and compared using the Mann-Whitney *U* test. For fibroatheroma and lesion-level data, a model with a generalized estimating equation approach was used to compensate for potential cluster effects of multiple lesions and fibroatheromas in the same patient and presented as least squares means with 95% confidence intervals (CI). Multivariate logistic regression analysis was used to determine independent predictors of a plaque rupture. Since plaque rupture could influence IVUS-VH quantitative measures, the IVUS-VH parameters were not included in the analysis. Receiver-operating characteristic (ROC) analysis and calculation of sensitivity and specificity were performed to test the ability of location data and other grayscale parameters to differentiate ruptured fibroatheroma from nonruptured fibroatheroma. All statistical analyses were performed using SAS version 9.1.3 (SAS Institute Inc., Cary, North Carolina). When 2 or more ROC curves were statistically significant, these curves were compared by MedCalc Statistical Software version 13.0 (MedCalc Software, Ostend, Belgium). A p value of <0.05 was considered statistically significant.

RESULTS

PATIENT CHARACTERISTICS. Baseline characteristics of the 454 patients with at least 1 nonculprit vessel fibroatheroma who were included in this analysis are shown in Table 1. The median age of the patients was 58.6 years, 80.2% were men, and 17.9% had diabetes mellitus. The prevalence of statin, aspirin, and clopidogrel use at admission was 46.7%, 72.7%, and 62.3%, respectively.

ANGIOGRAPHIC, GRAYSCALE, AND IVUS-VH FINDINGS. Patient-level and lesion-level angiographic, grayscale IVUS, and IVUS-VH results are listed in Table 2. Briefly, the median number of lesions per patient identified by angiography and IVUS was 2.0 and 5.0, respectively. In addition, 67.3% of patients had at least 1 TCFA-VH. Among 2,383 analyzed lesions, there were 18.9% with a minimum lumen area <4 mm^2 and 9.2% with a plaque burden ≥70%. In total, 74 ruptured fibroatheromas were identified, of which 90.5% (67 of 74) were located in a non-left main coronary location: 18.9% (14 of 74) were in the LAD, 17.6% (13 of 74) were in the LCX, and 54.1% (40 of 74)

were in the RCA. The frequency of plaque rupture was 1.7% (14 of 823), 2.2% (13 of 579), and 4.5% (40 of 898) in the LAD, LCX, and RCA, respectively ($p = 0.004$).

LONGITUDINAL DISTRIBUTION OF FIBROATHEROMAS IN NONCULPRIT VESSELS. Figure 1 illustrates fibroatheroma distribution every 10 mm axial distance from each coronary ostium. The majority of nonruptured and ruptured fibroatheromas were located in the proximal (43.4%) and middle (30.2%) segments. Nevertheless, the gradient from proximal to distal was least in the RCA, in which fibroatheromas (including plaque rupture) were distributed more evenly compared with the LAD and LCX.

Dividing the fibroatheromas into 4 groups based on the mean external elastic membrane (EEM) area (<10 mm^2, 10 to 15 mm^2, 15 to 20 mm^2, and >20 mm^2), fibroatheromas were more likely to be observed in segments with large vessel areas. Fibroatheromas were preferably located in proximal segment with larger vessels in the LAD and LCX. By contrast, the vessel area of the RCA did not differ as dramatically as did the LAD and LCX from the proximal to the distal segments; in the RCA the majority of the segments had an EEM area that was >15 mm^2. Therefore, fibroatheromas clustered in large proximal vessels in the LAD and LCX while they seemed to be distributed diffusely throughout the RCA (Figure 2). With respect to mean plaque burden, it was the smallest in the distal segment versus the proximal and middle segments in the LAD and RCA, but not in the LCX (Table 3).

PREDICTORS OF PLAQUE RUPTURE AMONG NONCULPRIT, NON-LEFT MAIN FIBROATHEROMAS. The following potential predictors of plaque rupture in the LAD, LCX, or RCA were assessed in the multivariate logistic regression model: mean EEM area, mean plaque burden, distance from ostium to maximum NC slice, calcium identified by grayscale IVUS, and RCA location. Pooling all non-left main fibroatheromas together, all of these variables were independent predictors of plaque rupture (Table 4). The more proximal the location and the larger the EEM area and plaque burden, the more likely plaque rupture was to develop.

According to the ROC analysis for the predictors of plaque rupture (Figure 3), among fibroatheromas in the LAD, LCX, or RCA, EEM area (area under the curve [AUC]: 0.78, $p < 0.001$) and plaque burden (AUC: 0.65; $p < 0.001$), but not the distance from ostium to the maximum NC site (AUC: 0.56; $p = 0.09$), could discriminate ruptured from nonruptured fibroatheromas. A threshold of EEM area >16.3 mm^2 and plaque burden >50% distinguished fibroatheromas with plaque ruptures from those without plaque rupture with a sensitivity of 88.1% and 83.6%, a specificity of 53.9% and 43.4%, a positive predictive value of 5.4% and 4.2%, a negative predictive value of 99.3% and 98.9%, and an accuracy of 54.7% and 44%, respectively. While comparing EEM area versus plaque burden versus longitudinal location, the distance from the ostium was the least predictive for plaque rupture (EEM vs. distance, $p < 0.001$; plaque burden

FIGURE 1 Longitudinal Distribution of Fibroatheromas and Plaque Rupture

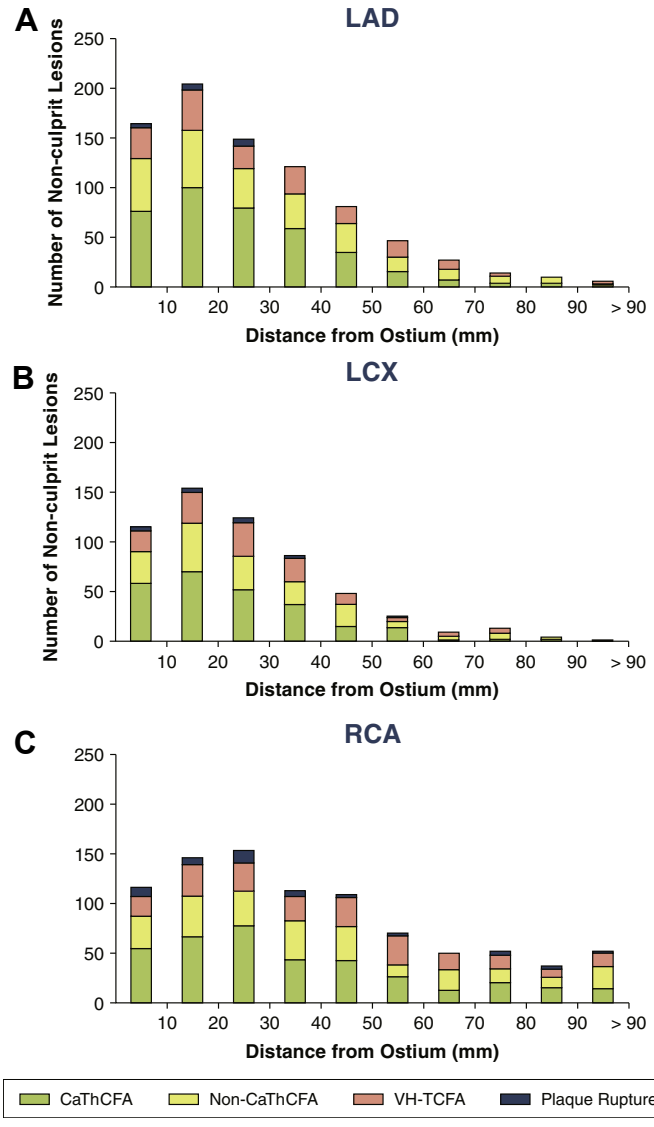

The y-axis represents number of advanced lesion characteristics. The x-axis indicates the length from the ostium of **(A)** left anterior descending artery (LAD), **(B)** left circumflex artery (LCX), and **(C)** right coronary artery (RCA). CaThFCA = calcified thick-cap fibroatheroma; Non-CaThCFA = noncalcified thick-cap fibroatheroma; VH-TCFA = thin-cap fibroatheroma detected by virtual histology-intravascular ultrasound.

FIGURE 2 Spatial Distribution of Fibroatheromas of Different Vessel Area

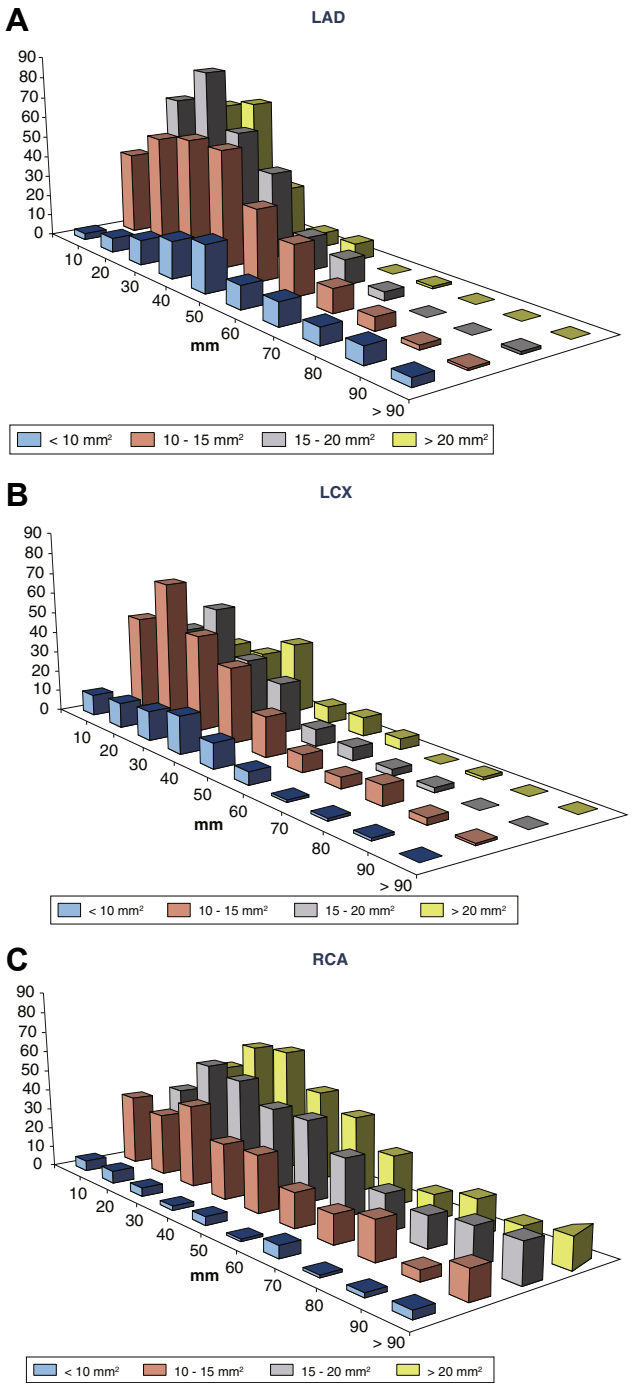

The x-axis represents the distance from the ostium of each coronary artery (in mm) to the maximum NC site within each fibroatheroma. **Blue**, **pink**, **gray**, and **yellow** bars represent fibroatheromas with external elastic membrane areas of <10 mm², 10 to 15 mm², 15 to 20 mm², and >20 mm², respectively. The y-axis indicates the absolute number of fibroatheromas according to distance from the coronary ostium and external elastic membrane area. LAD = left anterior descending artery; LCX = left circumflex artery; RCA = right coronary artery.

vs. distance, p = 0.05) while the EEM area (compared with plaque burden) seemed to be a better predictor of plaque rupture (p < 0.001).

FIBROATHEROMAS AND RUPTURES IN THE LEFT MAIN CORONARY ARTERY. In total, 7 ruptured fibroatheromas and 163 nonruptured fibroatheromas were identified in the left main coronary artery (frequency of 4.1%) with a spatial distribution that was different from the other 3 coronary arteries. Most of the fibroatheromas (82.8%) were localized in the distal 10 mm segment of the left main artery. Ruptured fibroatheromas had a larger plaque area (15.6 mm² [95% CI: 12.7 to 16.8] vs. 11.4 mm² [95% CI: 9.3 to 13.4], p = 0.006) and plaque burden (59.6% [95% CI: 52.2 to 61.5] vs. 46.0% [95% CI: 40.2 to 52.6], p = 0.002), but similar vessel area (27.6 mm² [95% CI: 22.2 to 27.9] vs. 24.8 mm² [95% CI: 21.4 to 27.5], p = 0.24) and lumen area (10.8 mm² [95% CI: 9.8 to 15.0] vs. 13.1 mm² [95% CI: 10.6 to 15.2], p = 0.24) compared with nonruptured fibroatheromas; however, plaque burden was the only significant predictor (AUC: 0.85; p < 0.001) by ROC analysis. A cut-off value of plaque burden >59.2% discriminated plaque rupture from nonrupture with a sensitivity of 71.4%, a specificity of 92.6%, a positive predictive value of 29.5%, a negative predictive value of 98.7%, and an accuracy of 91.8%.

DISCUSSION

In the current study we assessed the longitudinal distribution of grayscale and IVUS-VH parameters among fibroatheromas in nonculprit coronary arteries, as well as the impact of vessel area and plaque burden on plaque rupture. The main findings are as follows: 1) there was a gradient of high-risk plaques (fibroatheromas of all types and plaque ruptures) from proximal to distal coronary segments, mainly in the LAD and LCX and least in the RCA; and 2) although proximal location was an independent predictor for plaque rupture, vessel area and plaque burden were better discriminants of plaque rupture versus nonruptured fibroatheromas rather than the distance from the ostium to the maximum NC site.

Previous autopsy, angiographic, IVUS, and optical coherence tomography studies elucidated that the majority of high-risk plaques including ruptured plaques accumulated in proximal segments of the coronary tree (5-8,15-17). Cheruvu et al. (5), Farb et al. (18), and Davies (19) have reported that most histopathologic TCFAs and plaque ruptures clustered in the proximal third of coronary arteries, mainly in the LAD and LCX. This was confirmed by subsequent IVUS and optical coherence tomography

TABLE 3 Volumetric Grayscale Analysis of Nonculprit Fibroatheromas in LAD, LCX, or RCA

	Proximal 0-20 mm	Middle 20-40 mm	Distal >40 mm	p Value
Mean EEM area, mm^3/mm				
Overall (n = 2,300)	16.64 (13.98-20.92)	15.90 (12.49-19.71)	15.07 (11.30-19.18)	<0.0001
LAD (n = 823)	17.24 (14.80-20.97)	14.97 (11.89-17.74)	11.21 (9.24-14.39)	<0.0001
LCX (n = 579)	15.00 (12.51-18.61)	13.99 (11.38-18.59)	13.26 (10.14-16.90)	0.004
RCA (n = 898)	17.51 (14.72-22.71)	18.36 (14.60-23.03)	17.36 (13.95-21.37)	0.02
Mean plaque area, mm^3/mm				
Overall (n = 2,300)	8.57 (6.97-10.80)	8.21 (6.35-10.43)	7.28 (5.53-9.92)	<0.0001
LAD (n = 823)	9.13 (7.67-11.08)	7.82 (6.27-9.61)	5.82 (4.57-7.41)	<0.0001
LCX (n = 579)	7.43 (6.03-9.27)	7.16 (5.43-9.19)	6.78 (5.42-9.46)	0.04
RCA (n = 898)	9.01 (6.98-11.25)	9.77 (7.61-12.53)	8.52 (6.56-10.71)	<0.0001
Mean lumen area, mm^3/mm				
Overall (n = 2,300)	7.22 (5.63-9.71)	7.13 (5.24-9.56)	7.52 (5.74-9.96)	<0.0001
LAD (n = 823)	8.00 (6.25-10.26)	6.47 (5.08-8.16)	5.45 (4.02-6.97)	<0.0001
LCX (n = 579)	7.50 (5.73-9.46)	6.93 (5.23-9.61)	6.38 (4.60-7.66)	0.0007
RCA (n = 898)	8.50 (6.47-11.68)	8.44 (6.34-11.52)	8.50 (6.48-11.36)	0.75
Plaque burden, %				
Overall (n = 2,300)	52.0 (45.8-57.6)	52.1 (46.4-59.0)	50.8 (44.7-56.9)	0.001
LAD (n = 823)	53.8 (47.4-59.4)	54.5 (48.6-60.1)	51.9 (45.7-58.7)	0.02
LCX (n = 579)	50.5 (44.6-56.4)	50.5 (44.8-55.2)	51.7 (47.3-57.5)	0.11
RCA (n = 898)	51.2 (45.0-56.9)	52.0 (45.6-59.4)	49.6 (43.2-55.2)	0.0005

Values are least squares means (95% confidence interval) or % (n).

EEM = external elastic membrane; IVUS = intravascular ultrasound; LAD = left anterior descending artery; LCX = left circumflex artery; RCA = right coronary artery; VH = virtual histology.

studies of the left coronary arteries, but these studies suggested a more uniform distribution in the RCA that was also observed in the current study (6-8). In addition, high-risk left main coronary artery plaque was more likely to occur close to the distal left main coronary artery bifurcation (20), as also seen in the current study.

Kotani et al. (21) reported that culprit lesions with plaque rupture had a larger EEM area and plaque mass than nonculprit lesions among patients with ST-segment elevation myocardial infarction. In addition, by using IVUS across the entire coronary arteries, Wykrzykowska et al. (8) and Golinvaux et al. (7) found a significant gradient of both EEM area and plaque burden from proximal to distal in the LAD but not in the RCA. Furthermore, the plaque burden and EEM area were much larger in the distal RCA compared with distal LAD (8). Larger vessel area with greater plaque burden was more likely to coexist with positive remodeling that has also been considered as a morphologic feature of vulnerable coronary disease (22-24). In the current study, EEM area (>17.1 mm^2) and plaque burden (>50%) were identified as independent risk factors of plaque rupture. Less anatomic tapering with potentially higher EEM volumes and plaque burden (both independent predictors for plaque burden in this analysis) may explain the more uniform distribution of high-risk fibroatheromas in the RCA. The power of the EEM area as a predictor of plaque rupture might be that it integrates vessel area, plaque burden, and positive remodeling, all of which may be important.

Disturbed coronary flow with low shear stress plays an important role in the pathogenesis of the atherosclerotic plaque that often develops near arterial bifurcations, branch ostia, and curvatures (25). Thus, the proximal segments of the LAD and LCX with major side branches promote the development of disturbed flow that could also occur near the distal left main coronary artery bifurcation. The absence of branches in the RCA may be another explanation for the diffuse distribution of high-risk plaques.

TABLE 4 Multivariate Logistic Regression Analysis Predictors for Plaque Rupture in LAD, LCX, or RCA

	Odds Ratio	95% CI	p Value
Distance from ostium to max NC site, per 10 mm	0.86	0.76-0.98	0.02
Mean external elastic membrane area, per mm^2	1.14	1.11-1.17	<0.0001
Mean plaque burden, per 10%	2.05	1.63-2.58	<0.0001
Calcium	0.09	0.05-0.18	<0.0001
RCA	2.16	1.25-3.27	0.006

CI = confidence interval; max NC = maximum necrotic core; LAD = left anterior descending artery; LCX = left circumflex artery; RCA = right coronary artery.

FIGURE 3 Receiver-Operating Characteristic Analysis of Predictors for Plaque Rupture Among Nonculprit Fibroatheromas

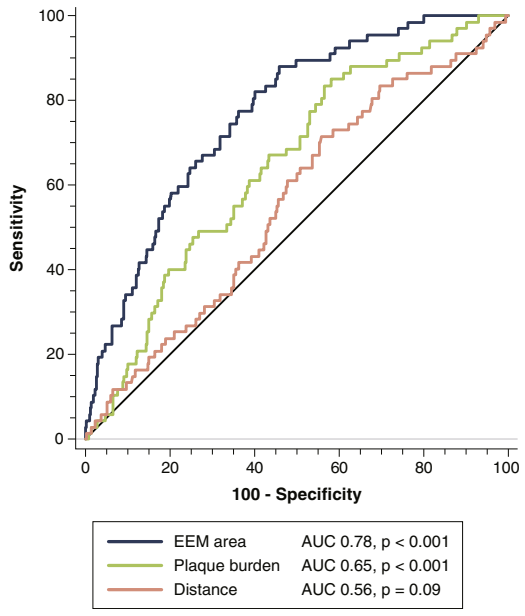

Both external elastic membrane (EEM) and plaque burden distinguished ruptured fibroatheromas from those without plaque rupture, but not the distance from the ostium to the maximum necrotic core site among fibroatheromas in left anterior descending coronary arteries, left circumflex arteries, and right coronary arteries. EEM area versus distance, $p < 0.001$; plaque burden versus distance, $p = 0.05$; EEM area versus plaque burden, $p < 0.001$.

In the present study, there was a preponderance of FA plaque ruptures in the RCA. There are a number of possible explanations. One is that FA ruptures in the LAD or in a large LCX may more likely be immediately fatal. Another explanation is that the RCA is longer, larger, tapers less, has a larger plaque burden, and is typically diffusely diseased over a longer segment (i.e., ostium to distal bifurcation) compared to the LAD or LCX (26); therefore, there are more potential sites for the development of a rupture-prone FA.

STUDY LIMITATIONS. First, in the current analysis, patients were enrolled after successful percutaneous coronary intervention treatment of the culprit lesion(s); culprit lesions were not included in the current analysis. Second, most of the analysis was performed at the fibroatheroma level; however, non-fibroatheromas are less likely to lead to cardiac events (27). Third, due to the fact that plaque rupture could affect the quantitative IVUS-VH data, the multivariate logistic regression model did not include IVUS-VH parameters. Finally, side branches were not studied.

CONCLUSIONS

The current analysis from the PROSPECT study demonstrated that plaque rupture was associated with larger vessel area, greater plaque burden, and proximal location within nonculprit coronary arteries; however, EEM area was the strongest predictor for plaque rupture in the LAD, LCX, and RCA, while plaque burden seemed to be the most important risk factor for plaque rupture in the left main coronary artery.

REPRINT REQUESTS AND CORRESPONDENCE: Dr. Akiko Maehara, Cardiovascular Research Foundation, 111 East 59th Street, 12th Floor, New York, New York 10022. E-mail: amaehara@crf.org.

PERSPECTIVES

COMPETENCY IN MEDICAL KNOWLEDGE: Among nonculprit lesions of patients with acute coronary syndromes who were enrolled in the PROSPECT study, proximal lesion location, increasing vessel size, and plaque burden detected by grayscale IVUS were more likely to be associated with plaque rupture. In addition, larger vessel area (EEM >16.3 mm^2) was the best marker for plaque rupture in non–left main lesions; and a greater plaque burden (>60%) was the best marker of ruptured plaque in left main lesions.

TRANSLATIONAL OUTLOOK: Further investigations are needed to validate these findings, especially the influence of vessel size on plaque rupture and the value of grayscale IVUS parameters in predicting plaque rupture and future cardiovascular events.

REFERENCES

1. Davies MJ, Thomas A. Thrombosis and acute coronary-artery lesions in sudden cardiac ischemic death. N Engl J Med 1984;310:1137–40.

2. Falk E, Shah PK, Fuster V. Coronary plaque disruption. Circulation 1995;92:657–71.

3. Shah PK. Mechanisms of plaque vulnerability and rupture. J Am Coll Cardiol 2003;41:15S–22S.

4. Virmani R, Burke AP, Farb A, et al. Pathology of the vulnerable plaque. J Am Coll Cardiol 2006;47:C13–8.

5. Cheruvu PK, Finn AV, Gardner C, et al. Frequency and distribution of thin-cap fibroatheroma and ruptured plaques in human coronary arteries: a pathologic study. J Am Coll Cardiol 2007;50:940–9.

6. Fujii K, Kawasaki D, Masutani M, et al. OCT assessment of thin-cap fibroatheroma distribution in native coronary arteries. J Am Coll Cardiol Img 2010;3:168–75.

7. Golinvaux N, Maehara A, Mintz GS, et al. An intravascular ultrasound appraisal of atherosclerotic plaque distribution in diseased coronary arteries. Am Heart J 2012;163:624–31.

8. Wykrzykowska JJ, Mintz GS, Garcia-Garcia HM, et al. Longitudinal distribution of plaque burden and necrotic core-rich plaques in nonculprit lesions of patients presenting with acute coronary syndromes. J Am Coll Cardiol Img 2012;5:S10–8.

9. Ojha M, Leask RL, Butany J, et al. Distribution of intimal and medial thickening in the human right coronary artery: a study of 17 RCAs. Atherosclerosis 2001;158:147–53.

10. Farmakis TM, Soulis JV, Giannoglou GD, et al. Wall shear stress gradient topography in the normal left coronary arterial tree: possible implications for atherogenesis. Curr Med Res Opin 2004;20:587–96.

11. Cunningham KS, Gotlieb AI. The role of shear stress in the pathogenesis of atherosclerosis. Lab Invest 2005;85:9–23.

12. Stone GW, Maehara A, Lansky AJ, et al. A prospective natural-history study of coronary atherosclerosis. N Engl J Med 2011;364:226–35.

13. Maehara A, Cristea E, Mintz GS, et al. Definitions and methodology for the grayscale and radiofrequency intravascular ultrasound and coronary angiographic analyses. J Am Coll Cardiol Img 2012;5:S1–9.

14. Xie Y, Mintz GS, Yang J, et al. Clinical outcome of nonculprit plaque ruptures in patients with acute coronary syndrome in the PROSPECT study. J Am Coll Cardiol Img 2014;7:397–405.

15. Toutouzas K, Karanasos A, Riga M, et al. Optical coherence tomography assessment of the spatial distribution of culprit ruptured plaques and thin-cap fibroatheromas in acute coronary syndrome. EuroIntervention 2012;8:477–85.

16. Antoni ML, Yiu KH, Atary JZ, et al. Distribution of culprit lesions in patients with ST-segment elevation acute myocardial infarction treated with primary percutaneous coronary intervention. Coron Artery Dis 2011;22:533–6.

17. Hong MK, Mintz GS, Lee CW, et al. A three-vessel virtual histology intravascular ultrasound analysis of frequency and distribution of thin-cap fibroatheromas in patients with acute coronary syndrome or stable angina pectoris. Am J Cardiol 2008;101:568–72.

18. Farb A, Tang AL, Burke AP, et al. Sudden coronary death. Frequency of active coronary lesions, inactive coronary lesions, and myocardial infarction. Circulation 1995;92:1701–9.

19. Davies MJ. Anatomic features in victims of sudden coronary death. Coronary artery pathology. Circulation 1992;85:I19–24.

20. Kim SW, Mintz GS, Weissman NJ, et al. Frequency and evolution of thin-capped fibroatheromas in left main coronary artery as assessed by serial virtual histology intravascular ultrasound analysis. J Invasive Cardiol 2014;26:175–9.

21. Kotani J, Mintz GS, Castagna MT, et al. Intravascular ultrasound analysis of infarct-related and non-infarct-related arteries in patients who presented with an acute myocardial infarction. Circulation 2003;107:2889–93.

22. Hong YJ, Jeong MH, Choi YH, et al. Positive remodeling is associated with vulnerable coronary plaque components regardless of clinical presentation: virtual histology-intravascular ultrasound analysis. Int J Cardiol 2013;167:871–6.

23. Schoenhagen P, Ziada KM, Kapadia SR, et al. Extent and direction of arterial remodeling in stable versus unstable coronary syndromes: an intravascular ultrasound study. Circulation 2000;101:598–603.

24. Prati F, Pawlowski T, Gil R, et al. Stenting of culprit lesions in unstable angina leads to a marked reduction in plaque burden: a major role of plaque embolization? A serial intravascular ultrasound study. Circulation 2003;107:2320–5.

25. Resnick N, Yahav H, Shay-Salit A, et al. Fluid shear stress and the vascular endothelium: for better and for worse. Prog Biophys Mol Biol 2003;81:177–99.

26. Kaple RK, Maehara A, Sano K, et al. The axial distribution of lesion-site atherosclerotic plaque components: an in vivo volumetric intravascular ultrasound radio-frequency analysis of lumen stenosis, necrotic core and vessel remodeling. Ultrasound Med Biol 2009;35:550–7.

27. Dohi T, Mintz GS, McPherson JA, et al. Non-fibroatheroma lesion phenotype and long-term clinical outcomes: a substudy analysis from the PROSPECT study. J Am Coll Cardiol Img 2013;6:908–16.

KEYWORDS fibroatheroma, intravascular ultrasound, plaque rupture